Comparison of classification methods with "*n*-class" receiver operating characteristic curves: a case study of energy drinks

Anita Rácz[1,2], Dávid Bajusz[3], Marietta Fodor[2], Károly Héberger[1,*]

[1] Plasma Chemistry Research Group, Research Centre for Natural Sciences, Hungarian Academy of Sciences, H-1117 Budapest XI., Magyar tudósok körútja 2, Hungary

[2] Corvinus University of Budapest, Faculty of Food Science, Department of Applied Chemistry, H-1118 Budapest XI., Villányi út 29-43, Hungary

[3] Medicinal Chemistry Research Group, Research Centre for Natural Sciences, Hungarian Academy of Sciences, H-1117 Budapest XI., Magyar tudósok körútja 2, Hungary

* To whom correspondence should be sent:

E-mail address: heberger.karoly@ttk.mta.hu (Károly Héberger)

Abstract

Four classification methods were compared using receiver operating characteristic (ROC) curves to identify the best one: two common ones (linear discriminant analysis, LDA and partial least squares, PLS) and another two (random forest, boosted tree) that are not applied as frequently as LDA or PLS yet. A dataset with 90 commercially available (in Hungary) energy drink samples were studied. Near-infrared (NIR) spectra were utilized for the classification of the energy drinks into three "natural" groups based on their sugar content. Another dataset, which contained the first ten principal components (PCs) was also used because of the limitation in the number of variables for LDA. The models were validated using *n*-fold cross-validation and randomization test. A new practice was elaborated to compare the pattern recognition methods with ROC curves. This new methodology was designed to provide an easy and straightforward way for the calculation of ROC curves for multi-class classification problems.

In each case the energy drink samples could be classified to the appropriate groups very accurately. The best ROC curve belonged to the boosted tree method, but all of the studied methods were able to classify the samples to a great extent of correctness. The use of AUC values instead of correct classification rates can be a viable option for method comparison and also as a classification parameter.

Keywords: classification, ROC curves, PCA, LDA, PLS, Random forest, Boosted tree, method comparison

Introduction

Originating from the field of radar detection [1,2], ROC curves (and area under the ROC curve, or AUC values) have become standard evaluation tools of classifier methods in several fields [3,4] (of which virtual screening is the one that inspired us to apply it in the present work) [5]. Probably the greatest advantage of the concept is that it encapsulates the whole set of solutions (*i.e.* classifier thresholds) to a binary classification problem, and thus gives an overall picture of the performance of the classifier method. Its greatest limitation however, is that it cannot be readily applied to problems related to multiclass classification.

Recently, much effort has been dedicated to introducing ROC curves and AUC values to the domain of multiclass classification. Some of these extensions are referred to as ROC hypersurfaces, and similarly, the generalization of AUC becomes the volume under the ROC hypersurface (VUS). To our knowledge, the earliest implementation is Mossman's three-way ROC surface for three-class problems. [6] In his approach, the VUS value corresponds to the probability that a randomly chosen trio of items (one from each class) is classified correctly. The VUS concept was further elaborated by Ferri and coworkers, who identified the trivial classifiers, minimum and maximum VUS values and their polytopes for an arbitrary set of binary classifiers [7]. For the visualization of higher-dimension ROC surfaces, many alternatives exist as detailed by Fieldsend and Everson [8], such as parallel coordinated graphs [9], self-organising maps [10], or the recently introduced cobweb representation of Diri and Albayrak [11]. Most approaches to the generalization of the ROC concept involve the deduction of the many-class problem to a set of two-class problems and summarizing the results. In 2001, Hand and Till elaborated a deduction method based on averaging the results of pairwise comparisons [12]. Their approach was later further elaborated by Landgrebe and Duin [13,14]. Also in 2001, a slightly different approach was taken by Provost and Domingos [15]: they calculated a weighted average of the AUC values obtained by taking each class as the reference (positive) class in turn, where the weight of a class's AUC value was that class's frequency in the dataset. A significant advantage of this method over pairwise ROC analysis is the computational cost: $O(n)$ *vs*. the $O(n^2)$ cost of pairwise analysis. A comparison of ROC generalization approaches for three-class problems was carried out in 2005 by Patel and Markey [16].

In this work, we have applied and elaborated on the one-versus-all approach of Provost and Domingos [15]. We provide an easy visualization method based on the formula of Hanley and McNeil for "ROC-like" curves [3], and apply the formula of DeLong and coworkers [17] and the law of error propagation [18] to estimate the total variance that is associated with the given classifier method. We believe that the methodology presented here is widely applicable for the quick, easy and statistically correct ROC analysis and visualization of multi-class classification problems.

In the chemometrics field user friendly tutorials are available *e.g.* in ref. [19]. They have also shown how to determine confidence intervals on the various measures. The authors of reference [20] use different conventions and the positive-negative encoding of classes is straightforward. (It contains some errors in formulas though).

Our approach is similar to the basic concept of a chemometric technique called soft independent modeling of class analogy (SIMCA) where each class is modeled one at a time and independently from each other [21]. SIMCA belongs to the group of class modeling techniques; some authors term it one-class classification. [22]

"The application of an algorithm to different types of data may result in diverse outputs, and in general, no single algorithm is optimal for solving all problems. Each set of chemical data therefore requires the choice of an optimal (or a near-optimal) algorithm for that particular data set" [23]. Therefore a variety of supervised pattern recognition techniques is worth to be tested [24].

Our aims were to (i) classify the groups of energy drinks, (ii) make good models for further prediction and most importantly (iii) find a new way to compare the pattern recognition methods with ROC curves. For this purpose we had to develop a new methodology for creating ROC curves for more than two classes, which can be useful in other similar cases too.

Materials and methods

Principal component analysis (PCA)

Principal component analysis is one of the most common pattern recognition techniques nowadays and it has had great success since the '80s and '90s. As an unsupervised technique, it cannot be used as a typical classification method, but it helps to identify some patterns (groupings, outliers, etc.) in the dataset without the classification of the samples.

PCA works as a dimension reduction method and the basic idea is that "latent variables" are created by the linear combination of the original variables. In other words the original data matrix can be decomposed to the product of two matrices: the score ($\boldsymbol{T}$) and loading ($\boldsymbol{P}^{\boldsymbol{T}}$) matrices, which are orthonormal. Here we calculated principal components (scores vectors). The principal components (scores) with larger eigenvalues contain the most important information from the original data matrix and with the use of these components, dominant patterns and groupings can be revealed. [25]

Linear discriminant analysis (LDA)

Linear discriminant analysis is a very useful and well-known classification method; it is a supervised technique (*i.e.* we have to know the class membership before the analysis). It is similarly a dimension reduction technique like PCA, but here we calculate canonical variables (latent variables, roots). Ellipsoids (or hyperellipsoids) can be plotted around the scattered points and the discriminant function is given by the line (or space), which is defined by the intersection of two ellipses. It is assumed that the variances of all classes are equal. In the case of *N* classes, the number of the canonical variables will be *N-1*.

There are several opportunities to choose the important or informative variables for the model building. In this study all variables, forward stepwise, backward stepwise and best subset selection methods were used for this purpose. The algorithm is described in detail in ref. [26].

Random forest [27]

Random forest is a tree-based method, which can be used for classification and regression problems alike. The basic idea is that it builds many trees and each of them predicts a classification. The final classification is made by a voting of the sequences of trees. The training algorithm for random forests applies the general technique called “bagging”, which is actually an aggregating technique. The trees are weak predictors, but together they produce an ensemble; with the vote of each tree, the method can make good predictions. The two main parameters that are to be optimized are the number of predictor variables and the number of trees. In this work, we have generally selected the lowest predictor number where the inclusion of more predictors did not visibly change the CC% rates (*i.e.* where the CC% reached a plateau). The number of trees was determined afterwards for the given predictor number in a similar manner.

Boosted tree

Boosting was originally defined for classification problems and later extended to regression ones. Boosted trees also build binary trees similarly to bagging trees: *i.e.* they partition the data into two parts at each split node. At each step of the boosting a simple (best) partitioning of the data is determined, and the deviations of the observed values from the respective means (residuals for each partition) are computed. While this is quite straightforward for regression, in the case of classification problems, the task is split into *n* sub-tasks (where *n* is the number of classes) and a logistic transformation is carried out to compute the (weighted) misclassification rates for subsequent boosting steps, and later, the final misclassification rates. [28] An important feature of boosted trees is the weighting of the samples based on the difficulty of correct classification: misclassified samples will be penalized in subsequent steps.

In case of stochastic gradient boosting: Each consecutive simple tree is to be built for only a randomly selected subsample of the full dataset ("training set"). The introduction of a certain degree of randomness into the analysis in this manner can serve as a powerful safeguard against overfitting (since each consecutive tree is built for a different sample of observations), and yield models (additive weighted expansions of simple trees) that generalize well to new observations, *i.e.*, exhibit good predictive character. The algorithm is described in detail in ref. [28].

PLS-DA

Partial least squares projections to latent structures or more commonly partial least squares is a regression method developed for many collinear variables: it works even if the number of variables exceeds the number of samples considerably. PLS can be thought of as a generalization of multiple linear regression, and it is statistically more robust. PLS provides regression coefficients, predicted Y values, and a set of scores and loading plots for better interpretation of models. The performance parameters providing a measure about the goodness of models are similar to those of MLR (square of the correlation coefficients, root mean squared error for calibration and validation). PLS forms new, so-called latent, variables as linear combination of the original ones (including the independent variable, Y) and used the new latent variables (scores) as predictors for Y [29]. The PLS algorithm can be easily understood from the tutorial: [30]. PLS can be used for solving discrimination problems [31] but the enhanced possibility of random classification should be kept in mind [32].

Receiver Operating Characteristic curves

Let's assume we have a continuous binary classifier B; the classes are encoded by + and – . We estimate the probability of a sample belonging to Class 1 (in other words, the probability of the sample encoded as positive). What is the threshold value of B, above which we should consider a sample positive? For every value of B, we can calculate the true positive rate TPR, the ratio of correctly classified positives to all positives; and the false positive rate FPR, the ratio of falsely classified negatives to all negatives. The ROC curve is created by plotting the TPRs against the FPRs for each (decreasing) threshold value, spanning a monotonically increasing curve from (0;0) to (1;1), as illustrated by the black stepwise curve in **Figure 1**.

On ROC curves, the (0;0) to (1;1) diagonal corresponds to random classification: any method whose ROC curve runs "over" the diagonal is better than random classification while methods with ROC curves "under" the diagonal are worse. In this sense, ROC curves give a quick visual comparison of classification methods. Their performances however, can be more accurately quantified with the area under the ROC curve value (AUC). By definition, the AUC value is a number between 0 and 1 and corresponds to the probability that a randomly chosen positive sample is ranked higher than a randomly picked negative. It has been shown by Hanley that the AUC value is equivalent to the Mann-Whitney-Wilcoxon statistic (often termed U-statistic) [3] . Variances of the AUC values can be calculated based on the formulas by DeLong and coworkers [17]:

$$Var_{Total} = \frac{Var(p_{positive})}{N_{positive}} + \frac{Var(p_{negative})}{N_{negative}} \tag{1}$$

$$Var\left(p_{positive}\right) = \frac{1}{N_{positive}-1} \sum_{i=1}^{N_{positive}} (p_{i,positive} - AUC)^2 \tag{2}$$

$$Var\left(p_{negative}\right) = \frac{1}{N_{negative}-1} \sum_{j=1}^{N_{negative}} (p_{j,negative} - (1 - AUC))^2 \tag{3}$$

Here, *Var* means variance, *N* denotes sample sizes, while [$p_{i,positive}$/$p_{j,negative}$] are the (posterior) probabilities of each [positive/negative] scoring higher than a randomly chosen [negative/positive]. (The formulas are reproduced from ref. [33]).

By design, ROC curves are "stepwise", *i.e.* they consist of horizontal and vertical steps. Their unique and somewhat deceptive characteristic is that no independent variable is shown on them: TPR and FPR both depend on the classifier threshold B, which is "hidden". While methods exist for the fitting of ROC curves [34,35], they imply the use of advance curve-fitting techniques and are relatively scarcely used. On the other hand, production of "ROC-like" curves with a predefined AUC value is easily done with the formula presented recently by Nicholls [33] based on the work of Hanley and McNeil [3]:

$$Y = X^{\frac{1-AUC}{AUC}} \tag{4}$$

The colored curves in **Figure 1** are ROC curves calculated with the Hanley formula. In contrast to "real" ROC curves, they are not stepwise, nevertheless their shapes resemble "typical" ROC curves and thus they can make a handy tool for the quick visualization of classifier methods whose performances cannot be captured on a single ROC curve (such as multiclass classification methods).

Figure 1

n-Class ROC curves

Our approach to the multi-class ROC analysis of the three-class classification problem presented in this article is based on the one-versus-all method of Provost and Domingos [15]. Thus, we calculate AUC values by taking each class as positives (and all the others as negatives) in turn. The weighted average of these AUC values gives the overall AUC of the given classifier method:

$$\overline{AUC} = \frac{\sum_{i=1}^{n} N_i AUC_i}{\sum_{i=1}^{n} N_i} \qquad (5)$$

The weights N_i are the sample sizes of each class. We can visualize an overall ROC curve for a classifier method by plotting a “ROC-like” curve with the overall AUC value using the Hanley formula. The variance of the overall AUC value can be calculated with the law of error propagation [18]:

$$Var(\overline{AUC}) = \frac{\sum_{i=1}^{n} N_i^2 Var(AUC_i)}{\sum_{i=1}^{n} N_i^2} \qquad (6)$$

When comparing more classifier methods, ROC-like curves with AUCs corresponding to either confidence limits or the mean ± one SD of the overall AUC can also be plotted to decide whether the performances of the methods differ significantly. In this work, we plot curves corresponding to the mean ± one SD for the comparison of the methods.

Throughout this work, the classifiers that were used for ROC curve generation are class membership probabilities for LDA, Random forest and Boosted tree (the higher the better). For

PLS-DA, we have calculated for each sample the absolute differences between the predicted class (continuous) and the current "positive" class (discrete): here, a lower value is better. For example if we're plotting the ROC curve where we take "class2" objects as positives, an object with a predicted class of 1.8 will score better than another with a predicted class of 2.4, as the absolute difference will be abs(1.8 – 2) = 0.2 for the first one and abs(2.4 – 2) = 0.4 for the second one. For the other classes, ROC curves are generated in an identical manner, and afterwards the overall ROC and AUC are calculated from the class-specific ROC curves/AUC values as detailed above.

Results and discussion

Two datasets were applied for the further statistical analysis: the first one contained the 90 energy drink samples' spectral data and the second was calculated from the spectral data with principal component analysis. The results are discussed in two parts based on the used dataset. Both of the matrices had a categorical variable with the classes of the sugar contents. Usually, energy drinks contain sugar between zero and 15 g/100ml concentration. The reason of the splits is that there are commonly used amounts (for example 7,9 or 10,9 g/100ml) which are sometimes assigned to different blends, moreover it was interesting to notice that most of the producers tend to avoid sugar contents around 4-5 g/100ml and around 9 g/100ml. Thus we could split the dataset into three classes, which can be termed low, medium and high sugar content classes. The classification of the energy drinks with different methods was based on the three sugar content classes. As we can see later, not just the classification was the final purpose, but the comparison based on the predictive performance of each method with the use of probability values and ROC curves. In the plots the classes will be labeled as follows: class 1 = under 5 g/100ml; class 2= 5-10 g/100ml; class 3= above 10 g/100ml. The classification is somewhat arbitrary but it corresponds to the "natural" groupings of the samples.

I. Spectral dataset

In first case the dataset contained 90 samples and 649 spectral variables. The FT-NIR spectra were used between the range of 9000 and 4000 cm^{-1}. The spectra were recorded in transmission mode. Randomization test (Y-scrambling) and a systematic threefold cross-validation were used as validation methods in each case. Standardization was used as data pretreatment.

Results of partial least-squares discriminant analysis (PLS-DA)

For the proper comparison with other methods, the predicted values were used for the creation of ROC curves. First we wanted to determine the appropriate amount of PLS components (scores) for the classification. Five components were sufficient for the evaluation based on the PRESS values (predictive error of sum of squares, see Supplementary Figure S1). Though the three classes are close to each other **(Figure 2**), they can be separated with only a few samples being misclassified.

Figure 2

For the comparison of the correct classifications in the case of PLS-DA, all number of PLS components were used between one to ten to illustrate how the predictive capability changes with the use of more PLS scores. Thus, the ROC curves were created based on the predicted values in the case of each PLS component number. The creation of ROC curves was the same as described in the Materials and methods part. For every PLS component number, an average ROC curve was made with the use of the average AUC value of the three classes. **Figure 3** shows the final results of PLS-DA, where these average ROC curves for the ten PLS component numbers are plotted, along with the average curve of the ten cases. This latter curve can be a good option for the selection of the number of PLS components.

Figure 3

As we can see on **Figure 3**, the average of the ten ROC curves is near the curves for 4-5 components, which means that if we use five PLS components in this case, it will contain most of the predictive capability of our dataset and it won't provide an overfitted or an underfitted result, either. This component number is the same as given by PRESS values.

As we mentioned earlier, the predicted values for each sample were used for plotting ROC curves. This case was a little more specific than the cases of other methods. Here we use the predicted values in the following form: for each of the three classes we checked the nearest predicted value to the current exact class number, for instance for group three, the nearest one to three was searched. Then we continued with the second nearest one and so on, until we ordered all of the samples based on their distance from class three (see also the *"n*-class ROC curves" section). We have repeated it with the other two classes. Finally three ROC curves were created and for better comparison, the average of the AUC values of the three curves was used for the final evaluation. For plotting the latter one, the Hanley formula was applied, using the average AUC value. This average ROC curve can be used for the comparison with other methods' ROC curves. The five PLS component ROC curve was used for the comparison with other techniques.

Random forest (RF)

In the case of random forest, there were two parameters which could be optimized for better classification, namely the number of trees and the number of predictors. For this purpose the correct classification rates were calculated for each class in each combination of the parameters in the following way: first the number of trees was set to ten. It was smaller than the optimum, but we wanted to find the best predictor number with a smaller number of trees. Afterwards we have also optimized the number of trees for the determined predictor number. The most robust predictor number (based on the stabilization of classification rates for each group) was forty, where the correct classification rates (CC %) for groups 1, 2 and 3 were 0.96; 0.8077; 0.8718 respectively. We have selected the lowest predictor number where the inclusion of more predictors did not visibly change the CC% rates (*i.e.* where the CC% reached a plateau, see Supplementary Figure S2). It is also worth to note that there are some other options to determine the number of predictor variables, e.g. $\sqrt{M}$ or $\log_2(M+1)$ – where M is the total number of variables –, but these definitions work particularly for a smaller number of variables. Then the optimal number of trees was also determined. The best number of trees was thirty, after that the correct classification rates did not change (see earlier description and Supplementary Figure S3). The use of thirty trees leads to an increase of the CC % in the case of group 3 (0.8718 to 0.9487). Randomization and cross-validation were used for the validation of the classification model.

Instead of the correct classification rates, the probability values for each sample and group were used for plotting the ROC curves. The probability values were ordered by decreasing magnitude. The ROC curves of the three groups were averaged here too for the comparison with the other methods. **Figure 4** shows the ROC curves of the groups and the average of them.

Figure 4

Boosted tree

The boosted tree method is quite similar to the random forest technique, but here we had to optimize the number of trees and the number of tree size. For this purpose **Figure 5** clearly shows the global minimum of the average of multinomial deviance (calculated from the multinomial deviance loss function), which helped to choose the best parameter values for the classification.

Figure 5a,b

In our case the optimal number of the trees was 41 based on the average multinomial deviance of the test data (**Figure 5a**). The test set was randomly generated by bootstrapping a subset proportion of 50% (from the whole dataset) at each consecutive step. The maximum number of tree size was three. Cross-validation and a randomization test were also used in the validation step of the classification model building. **Figure 5b** clearly shows the difference for the randomized dataset, because the average multinomial deviance for the test data becomes larger with the use of more trees. (Usually a global minimum area should appear around the middle of the graph.)

As in the previous case, the probability values were used for the creation of ROC curves. **Figure 6** shows the three-group ROC curves and the average of them. It is really conspicuous that this method provides an almost perfect classification model. For better visibility, a magnified version of the ROC curves was used here.

Figure 6

Finally the average ROC curves of the three classification methods were plotted on the same figure to compare the final results and choose the best one. Five PLS components ROC curve, and the ROC curves for random forest and boosted tree are plotted on **Figure 7**, along with their average. Boosted tree was definitely the best one for the energy drink classification based on the sugar concentration.

Figure 7

Although the other two methods had worse outcomes, we can conclude that all of the used method can be good choices for the classification of energy drinks, their ROC curves are much better than the one for random classification. On the other hand it is worth to stress, that despite being not so frequently used, boosted tree can give reliable results, even improving upon those for LDA or PLS.

II. PCA scores dataset

In the second case the first ten scores of the principal component analysis were used for the classification and method comparison to overcome the problem of overfitting in LDA. These ten components were sufficient for the further evaluation, because they explained more than 99.7 % of the total variance in the dataset. This version was a more compressed one compared to the spectral dataset. In the following part we could see that it helped to improve all of the classification models and open new ways, because linear discriminant analysis (LDA) was also used with these datasets for the classification and method comparison. In the previous section we had to omit LDA, because the spectral dataset contained too many variables, and we did not want to leave out any of them.

Results of PLS-DA

In this section the main part of the evaluation was the same as in the spectral data's PLS-DA analysis. With the use of ten PCA scores, the plot of the R^2 and *PRESS* values was really simple. After two PLS scores, the values haven't changed much. It means that the first two PLS scores were sufficient for the statistical evaluation. On the other hand we wanted to see, whether it has a difference, if we plot all of the ten components on ROC curves. For this purpose, the predicted values in each case were used in the same way as for the spectral dataset and PLS-DA analysis. Randomization test and cross-validation were also used for the validation of the classification model. **Figure 8** shows the ROC curves with the use of different numbers of PLS scores. It is interesting to see that the curves do not change after two PLS components, which is also verified by the selection of the first two PLS components by PRESS values.

Figure 8

Random forest

For the selection of an appropriate number of trees and predictors, the number of predictors (1 to 8) and the number of trees (10 to 80) were plotted with the correct classification rates in each case. 3D surface plot was used for this with distance weighted least squares fitting. On **Figure 9** we can see this 3D graph, which clearly shows that the correct classification rates are increasing with the use of more trees and predictors, but only for a while. It is being quite constant around the middle of the plot and after seventy trees it has a little decrease. The selected parameters were thirty trees and five parameters, which can be seen on the beginning of the "acceptable region". These are the smallest parameters that we can use to get a good classification in the further evaluation. The correct classification rates were one of the highest in this case for each group.

Figure 9

With the use of appropriate parameters the classification model was built and the probability values for each groups and samples were applied for plotting the ROC curves. **Figure 10** shows the ROC curves of each groups and their average. All of the curves are far better than the use of random numbers, and if we take a look at the results, there is not much difference between using spectral data or principal component scores for random forest.

Figure 10

Boosted tree

In this section, two important parameters, namely the number of trees and the maximum tree size were optimized, as for the previous dataset. Here **Figure 11** shows the average multinomial deviance for train and test data as a function of the number of trees. It can be seen that the global minimum of the average multinomial deviance was 190 trees. This result suggests that there is an inverse relationship between the number of trees and the number of original variables, because for the spectral dataset the used number of trees was much lower (41) than here. Randomization test and cross-validation were used in the validation step.

Figure 11

After creating the classification model, ROC curves were plotted for the groups of energy drinks and their average AUC value. Probability values were used for the ROC curves (as for random forest). **Figure 12** shows the curves in a magnified version for better visualization. The plot is really interesting because it can be seen that both the average curve and the ROC curves of the groups had very high AUC values (almost 1.0), thus the classification in this case was outstanding.

Figure 12

Linear discriminant analysis (LDA)

The important variables for linear discriminant analysis were selected with backward and forward stepwise and best subset selection. Also, another model was built with all of the ten PCA scores. For best subset selection the limit of the variable number was five and Wilks' lambda statistic was used as the objective function. For forward stepwise and backward stepwise variable selection, we included/removed a variable if its inclusion/removal had a significant effect on the model at the 5% significance level (p to enter/remove = 0.05). Generally we can conclude that the three groups were classified quite well in all cases (forward stepwise, backward stepwise, best subset selection and all variables), which can be seen on **Figure 13**, where the two canonical scores (roots) are plotted against each other with the use of all of the ten original variables. The plot shows that LDA analysis with the PCA scores could compress the groups in comparison with PLS-DA with the spectral dataset. There are some misclassified samples, but their number is really low.

Figure 13

The results with the different selection methods were compared with the use of probability values in each group. The ROC curves were created based on the probability values as in the other cases, and plotted along with their average on **Figure 14**. The average values were also calculated with the same procedure as in the previous cases: The best classification model was created with the use of all variables, best subset selection was the second one and the forward and backward selections were the last one, but they also had very good AUC values.

Figure 14

In the final step a comparative plot with the average ROC curves of each classification model was plotted, which can be seen on **Figure 15**. All classification methods have very high AUC values, but the best one is without doubt the boosted tree method. It was also the best one in the case of the spectral dataset.

Figure 15

Conclusion

The application of the *n*-class ROC curves with the Hanley formula and weighted means can be a really good option for the comparison of classification methods. This approach can replace the correct classification rates as it can be applied in such cases when they are not available or require subjective input. Area under the ROC curve (AUC) values can be a good candidate as a correct classification metric; because they can be used anytime we have probability values or predicted values for each classified group members. Moreover the improved method can be applied for as many classes as one has, and the weighted average ROC curves will always give a good visual feedback and opportunity for comparison.

In the case study we could see that for both the spectral and the PCA scores datasets, boosted tree was the best method, but all of the methods can be used for the classification of energy drinks by their sugar content. Nowadays LDA and PLS-DA are more commonly used techniques than random forest and boosted tree, and a better result for instance with LDA was expected. In this point view we can conclude that one should try the less commonly used methods too (such as boosted tree), because they can give as good results as the common techniques, or even better if they are properly validated.

References

[1] W. Peterson, T. Birdsall, W. Fox, The theory of signal detectability, Trans. IRE Prof. Gr. Inf. Theory. 4 (1954) 171–212. doi:10.1109/TIT.1954.1057460.

[2] W.P. Tanner Jr., J.A. Swets, A decision-making theory of visual detection., Psychol. Rev. 61 (1954) 401–409. http://psycnet.apa.orgjournals/rev/61/6/401 (accessed July 1, 2015).

[3] J.A. Hanley, B.J. McNeil, The meaning and use of the area under a receiver operating characteristic (ROC) curve., Radiology. 143 (1982) 29–36. doi:10.1148/radiology.143.1.7063747.

[4] J. Swets, W.P. Tanner, T.G. Birdsall, Decision processes in perception., Psychol. Rev. 68 (1961) 301–340. doi:10.1037/h0040547.

[5] A.N. Jain, A. Nicholls, Recommendations for evaluation of computational methods., J. Comput. Aided. Mol. Des. 22 (2008) 133–9. doi:10.1007/s10822-008-9196-5.

[6] D. Mossman, Three-way ROCs, Med. Decis. Mak. 19 (1999) 78–89. doi:10.1177/0272989X9901900110.

[7] C. Ferri, J. Hernández-Orallo, M.A. Salido, Volume under the ROC Surface for Multi-class Problems, in: Mach. Learn. ECML 2003, Cavtat-Dubrovnik, Croatia, 2003: pp. 108–120.

[8] J.E. Fieldsend, R.M. Everson, Visualisation of multi-class ROC surfaces, in: ICML 2005 Work. ROC Anal. Mach. Learn., Bonn, Germany, 2005. https://ore.exeter.ac.uk/repository/handle/10871/11691.

[9] C.M. Fonseca, P.J. Fleming, Genetic Algorithms for Multiobjective Optimization: Formulation, Discussion and Generalization, in: Proc. Fifth Int. Conf. Genet. Algorithms, Morgan Kauffman, 1993: pp. 416–423. http://citeseer.ist.psu.edu/viewdoc/summary?doi=10.1.1.48.9077 (accessed July 3, 2015).

[10] T. Kohonen, Self-organising maps, Springer, 1995.

[11] B. Diri, S. Albayrak, Visualization and analysis of classifiers performance in multi-class medical data, Expert Syst. Appl. 34 (2008) 628–634. doi:10.1016/j.eswa.2006.10.016.

[12] D.J. Hand, R.J. Till, A simple generalization of the area under the ROC curve to multiple class classification problems, Mach. Learn. 45 (2001) 171–186.

[13] T. Landgrebe, R. Duin, A simplified extension of the area under the ROC to the multiclass domain, in: 17th Annu. Symp. Pattern Recognit. Assoc. South Africa, 2006: pp. 241–245.

http://scholar.google.com/scholar?hl=en&btnG=Search&q=intitle:A+simplified+extension+of+the+Area+under+the+ROC+to+the+multiclass+domain#0.

[14] T.C.W. Landgrebe, R.P.W. Duin, Approximating the multiclass ROC by pairwise analysis, Pattern Recognit. Lett. 28 (2007) 1747–1758. doi:10.1016/j.patrec.2007.05.001.

[15] F. Provost, P. Domingos, Well-Trained PETs: Improving probability estimation trees, 2001. doi:10.1.1.33.309.

[16] A.C. Patel, M.K. Markey, Comparison of three-class classification performance metrics: a case study in breast cancer CAD, in: M.P. Eckstein, Y. Jiang (Eds.), Med. Imaging, International Society for Optics and Photonics, San Diego, CA, USA, 2005: pp. 581–589. doi:10.1117/12.595763.

[17] E.R. DeLong, D.M. DeLong, D.L. Clarke-Pearson, Comparing the Areas under Two or More Correlated Receiver Operating Characteristic Curves: A Nonparametric Approach, Biometrics. 44 (1988) 837–845. http://www.jstor.org/stable/2531595?seq=1#page_scan_tab_contents (accessed June 23, 2015).

[18] H.H. Ku, Notes on the use of propagation of error formulas, J. Res. Natl. Bur. Stand. Sect. C Eng. Instrum. 70C (1966) 263–273. doi:10.6028/jres.070C.025.

[19] C.D. Brown, H.T. Davis, Receiver operating characteristics curves and related decision measures: A tutorial, Chemom. Intell. Lab. Syst. 80 (2006) 24–38. doi:10.1016/j.chemolab.2005.05.004.

[20] S.A. Shaikh, Measures Derived from a 2 x 2 Table for an Accuracy of a Diagnostic Test, J. Biom. Biostat. 2 (2011) 128. doi:10.4172/2155-6180.1000128.

[21] S. Wold, Pattern recognition by means of disjoint principal components models, Pattern Recognit. 8 (1976) 127–139. doi:10.1016/0031-3203(76)90014-5.

[22] R.G. Brereton, One-class classifiers, J. Chemom. 25 (2011) 225–246. doi:10.1002/cem.1397.

[23] D.H. Wolpert, W.G. Macready, No free lunch theorems for optimization, IEEE Trans. Evol. Comput. 1 (1997) 67–82. doi:10.1109/4235.585893.

[24] P.S. Gromski, E. Correa, A.A. Vaughan, D.C. Wedge, M.L. Turner, R. Goodacre, A comparison of different chemometrics approaches for the robust classification of electronic nose data, Anal. Bioanal. Chem. 406 (2014) 7581–7590. doi:10.1007/s00216-014-8216-7.

[25] S. Wold, K. Esbensen, P. Geladi, Principal component analysis, Chemom. Intell. Lab. Syst. 2 (1987) 37–52. doi:10.1016/0169-7439(87)80084-9.

[26] T. Hastie, R. Tibshirani and J. Friedman, Linear Discriminant Analysis, in: Elements of Statistical Learning. Data Mining, Inference, Prediction, Springer, New York, NY, USA, 2009: 2nd.ed., Chapter 4.3, pp. 106-119.

[27] L. Breiman, Random Forests, Mach. Learn. 45 (n.d.) 5–32. doi:10.1023/A:1010933404324.

[28] T. Hastie, R. Tibshirani and J. Friedman, Boosting trees, in: Elements of Statistical Learning. Data Mining, Inference, Prediction, Springer, New York, NY, USA, 2009: 2nd.ed., Chapters 10.5 and 10.6., pp. 345-350.

[29] R.G. Brereton, G.R. Lloyd, Partial least squares discriminant analysis: taking the magic away, J. Chemom. 28 (2014) 213–225. doi:10.1002/cem.2609.

[30] P. Geladi, B.R. Kowalski, Partial least-squares regression: a tutorial, Anal. Chim. Acta. 185 (1986) 1–17. doi:10.1016/0003-2670(86)80028-9.

[31] M. Barker, W. Rayens, Partial least squares for discrimination, J. Chemom. 17 (2003) 166–173. doi:10.1002/cem.785.

[32] K. Kjeldahl, R. Bro, Some common misunderstandings in chemometrics, J. Chemom. 24 (2010) 558–564. doi:10.1002/cem.1346.

[33] A. Nicholls, Confidence limits, error bars and method comparison in molecular modeling. Part 1: the calculation of confidence intervals., J. Comput. Aided. Mol. Des. 28 (2014) 887–918. doi:10.1007/s10822-014-9753-z.

[34] J.A. Hanley, The robustness of the “binormal” assumptions used in fitting ROC curves., Med. Decis. Mak. 8 (1988) 197–203. http://www.ncbi.nlm.nih.gov/pubmed/3398748 (accessed July 2, 2015).

[35] C.J. Lloyd, Fitting Roc Curves Using Non-linear Binomial Regression, Aust. N. Z. J. Stat. 42 (2000) 193–204. doi:10.1111/1467-842X.00118.

Caption to figures

Figure 1. A "real" ROC curve (black stepwise line) and four artificial ROC curves based on the Hanley-formula. (Note that the blue curve with AUC = 0.5 is identical to the diagonal.)

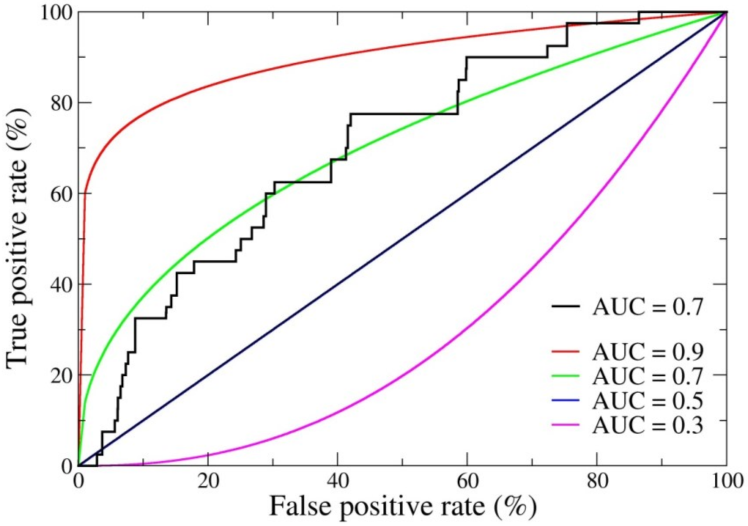

Figure 2: The second PLS component, plotted against the first PLS component.

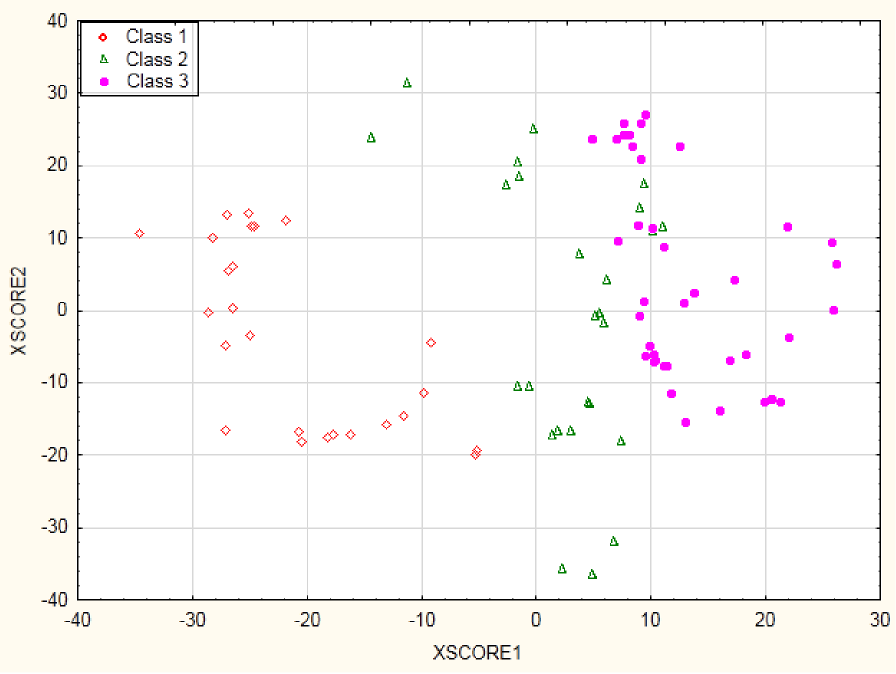

Figure 3: True positive rate plotted against false positive rate in the case of PLS-DA (spectral dataset). The graph is a magnified version of the original one (between 60 and 100 %) for better visibility. The AUC values increase with the number of PLS components from down to top.

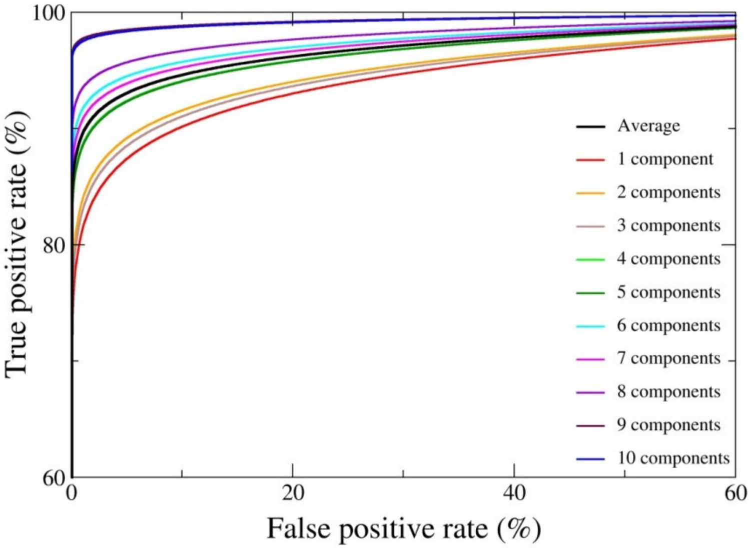

Figure 4: True positive rate plotted against false positive rate in the case of random forest (spectral dataset). Dashed lines indicate ± 1 SD from the average.

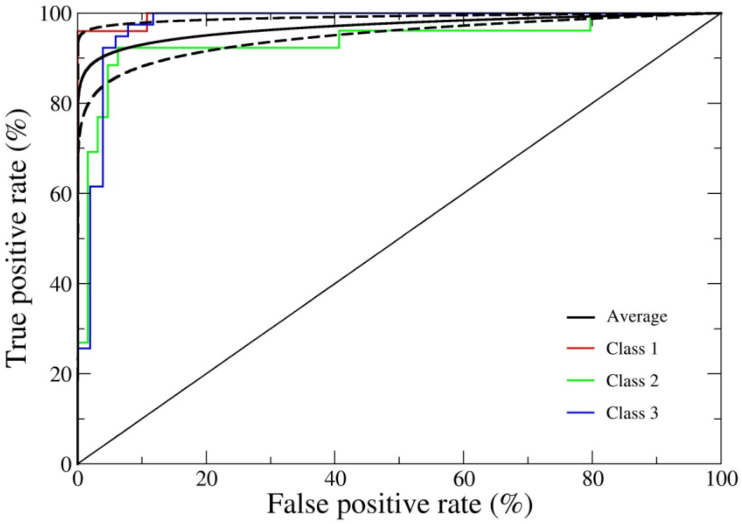

Figure 5a,b: The average multinomial deviance plotted against the number of trees for the original evaluation (a) and the randomized dataset (b). The optimal number is marked with a vertical line.

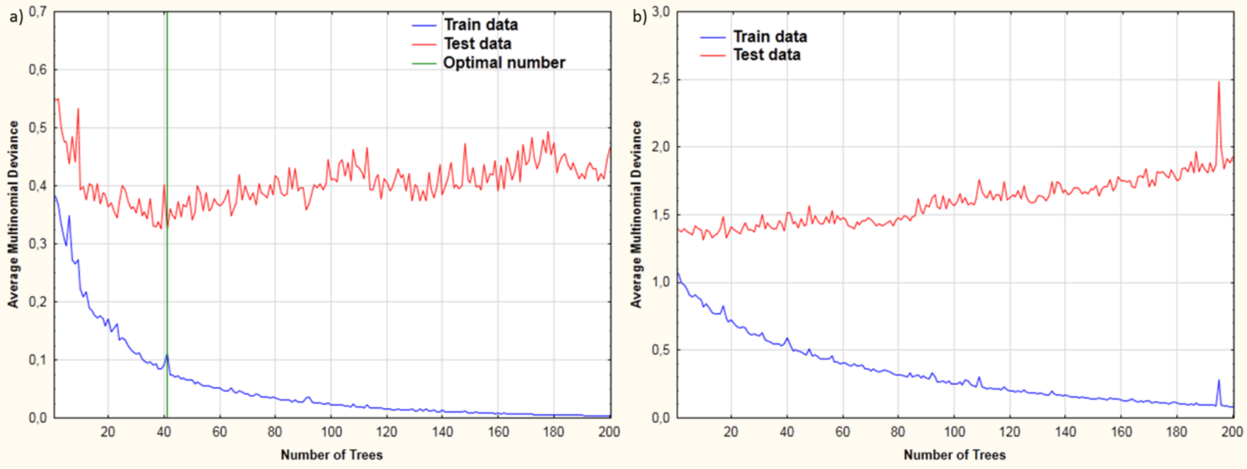

Figure 6: True positive rate, plotted against false positive rate for the boosted tree method (spectral dataset). The graph is a magnified version of the original one (between 60 and 100 %) for better visibility. Dashed lines indicate ± 1 SD from the average.

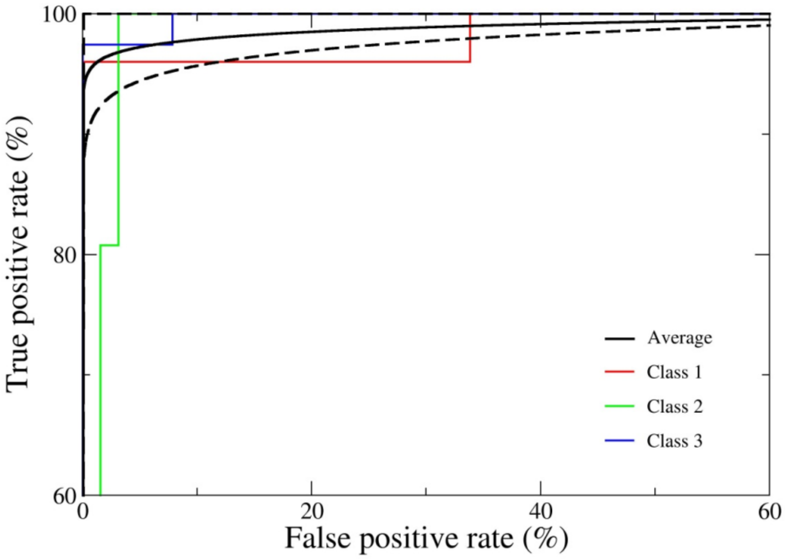

Figure 7: True positive rate, plotted against false positive rate in the case of all classification methods (spectral dataset). The graph is a magnified version of the original one (between 60 and 100 %) for better visibility. Dashed lines indicate ± 1 SD from the average. At this level of significance, boosted tree is significantly better than the average of the methods.

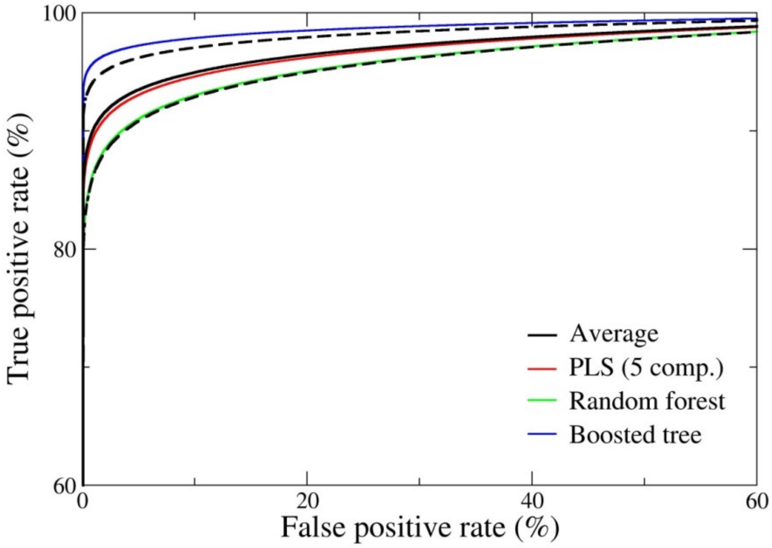

Figure 8: True positive rate plotted against false positive rate in the case of PLS-DA (PCA scores dataset). The graph is a magnified version of the original one (between 60 and 100 %) for the better visibility. The curves are really close to each other most of the time, thus they can't be differentiated in each case.

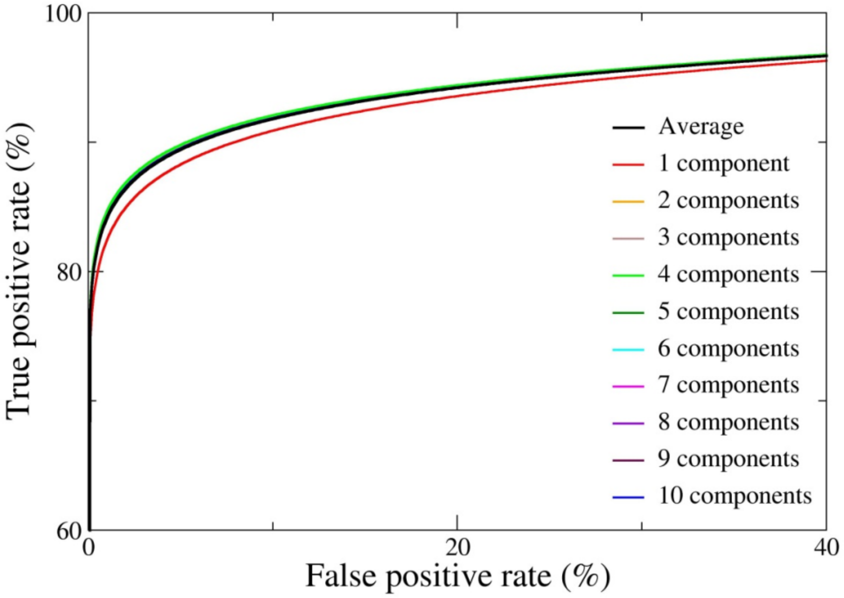

Figure 9: 3D plot of correct classifications, number of the trees and number of the predictors for the parameter selection for random forest. Distance weighted least squares fitting was used for the plot.

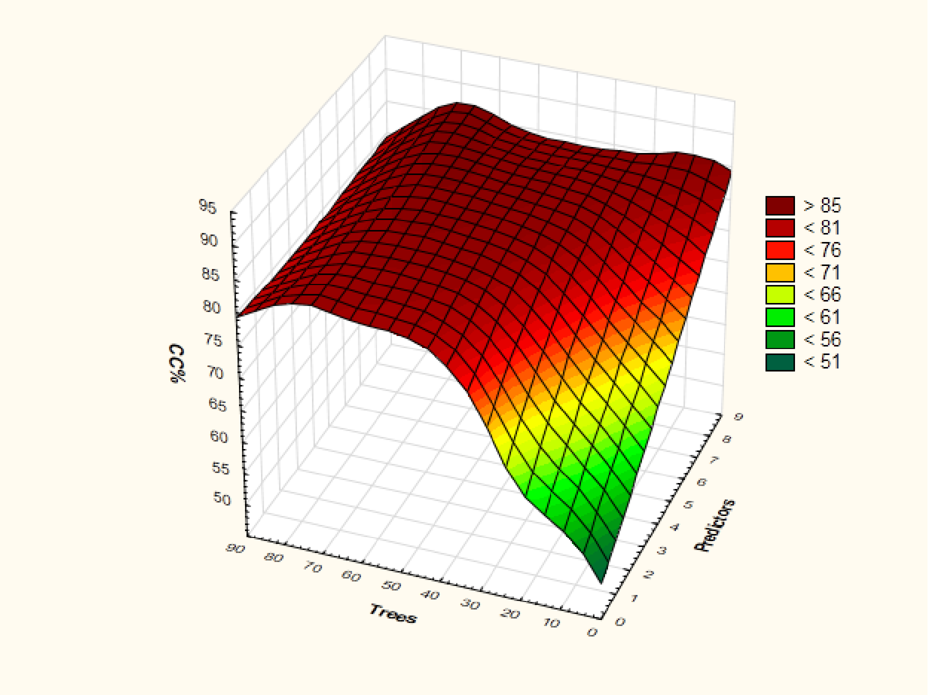

Figure 10: True positive rate plotted against false positive rate for random forest (PCA scores dataset). Dashed lines indicate ± 1 SD from the average.

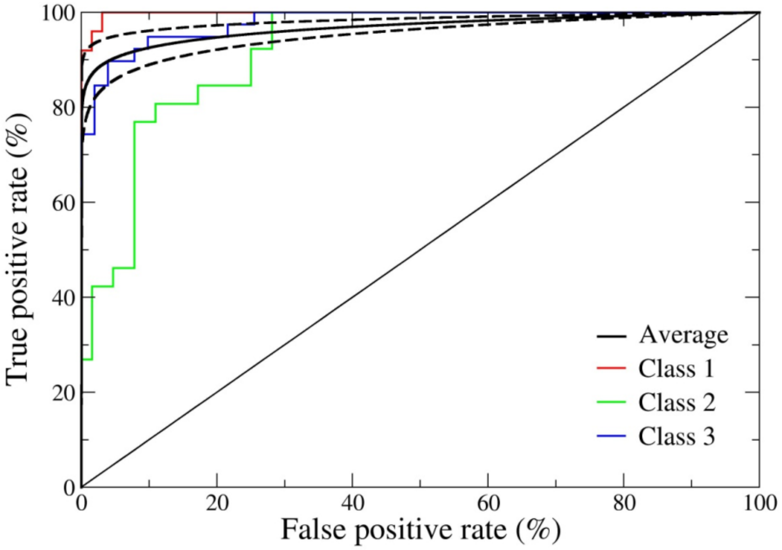

Figure 11: The average multinomial deviance was plotted against the number of trees in the case of boosted tree method (PCA scores dataset). The optimal number of trees is marked with vertical line.

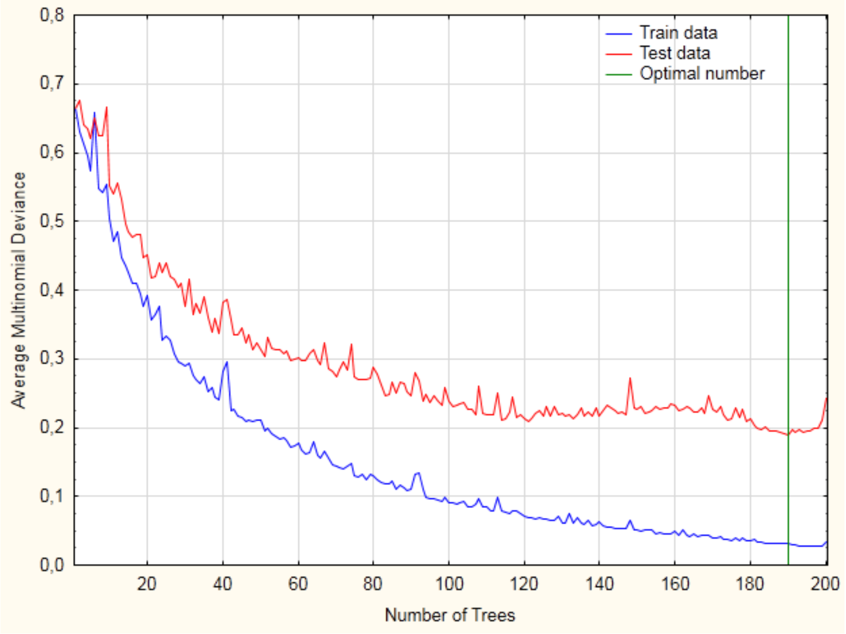

Figure 12: The true positive rate plotted against the false positive rate for boosted tree (PCA scores dataset). The plot is the magnified version of the original one for better visualization. Dashed lines indicate ± 1 SD from the average.

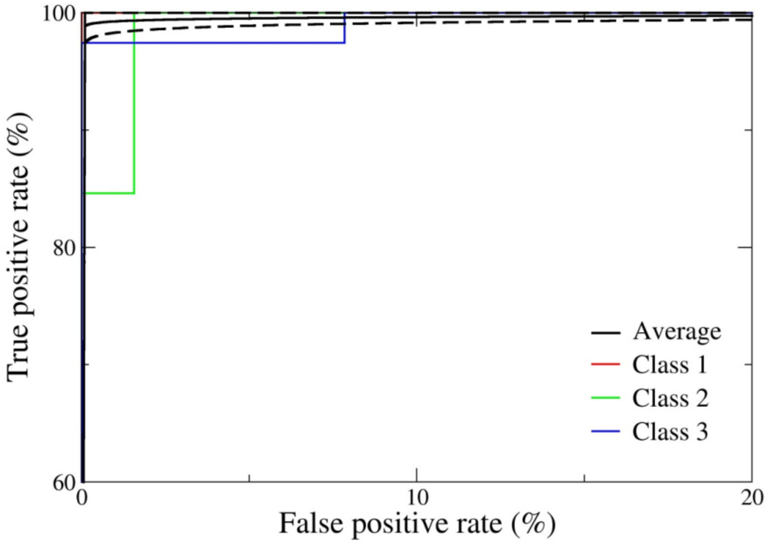

Figure 13: The LDA canonical scores (roots) are plotted against each other. The three examined energy drink groups are clearly separable.

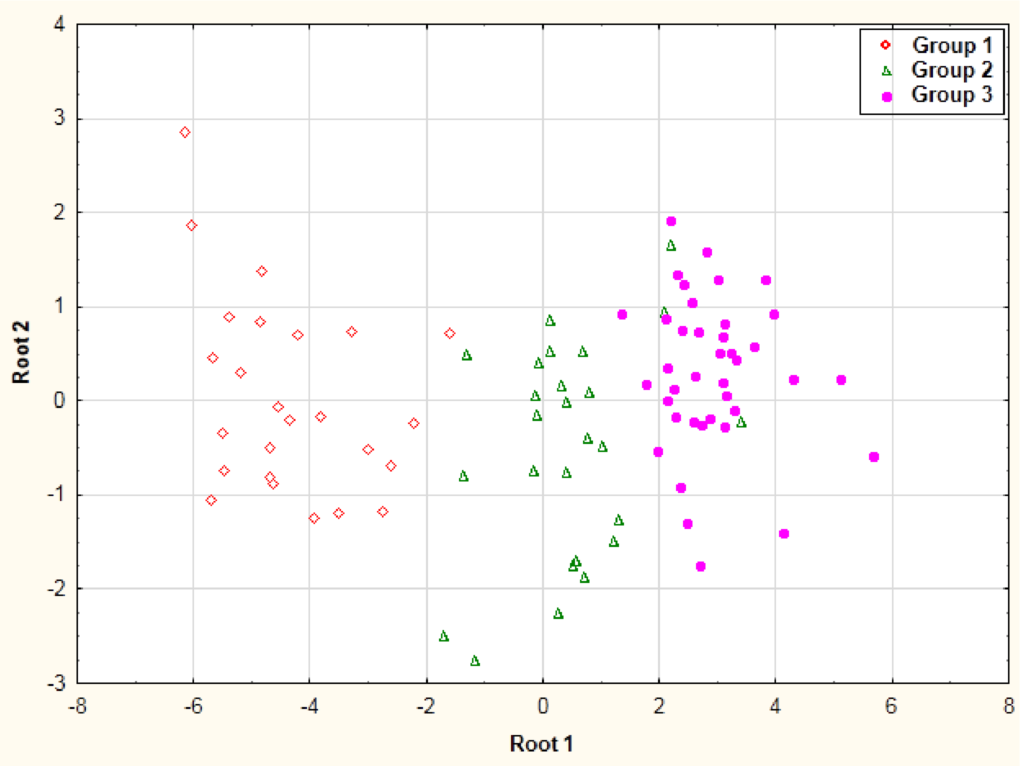

Figure 14: Comparison of the ROC curves with different variable selection methods. True positive rates are plotted against false positive rates. The plot is the magnified version of the original one for the better visualization. Dashed lines indicate ± 1 SD from the average. At this level of significance, using all variables performs significantly better than the average of the four approaches.

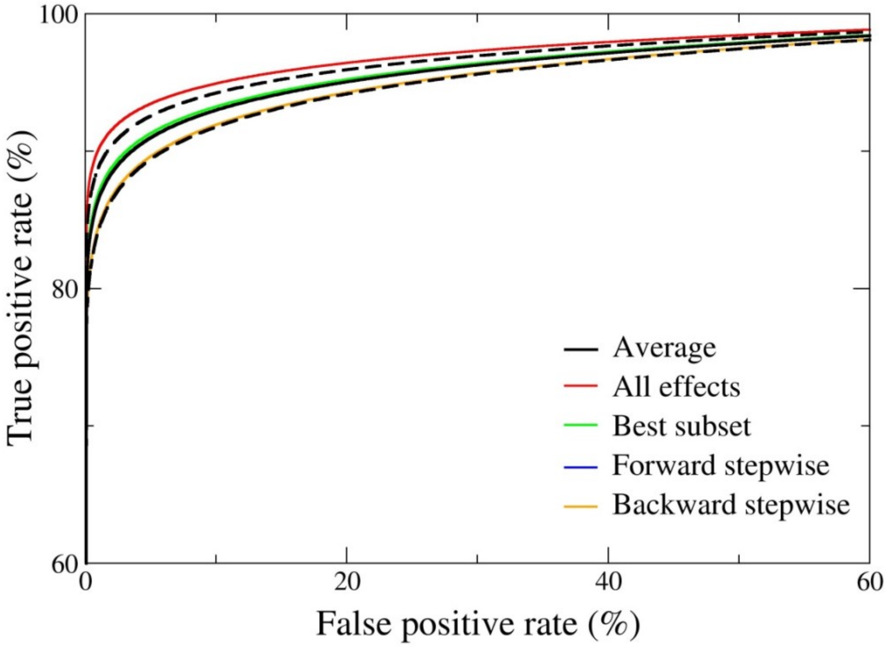

Figure 15: The final comparison of the four used classification methods for the PCA scores dataset. The plot is the magnified version of the original one for better visualization. Dashed lines indicate ± 1 SD from the average. At this level of significance, boosted tree is significantly better than the average, while all other methods can be considered equivalent.

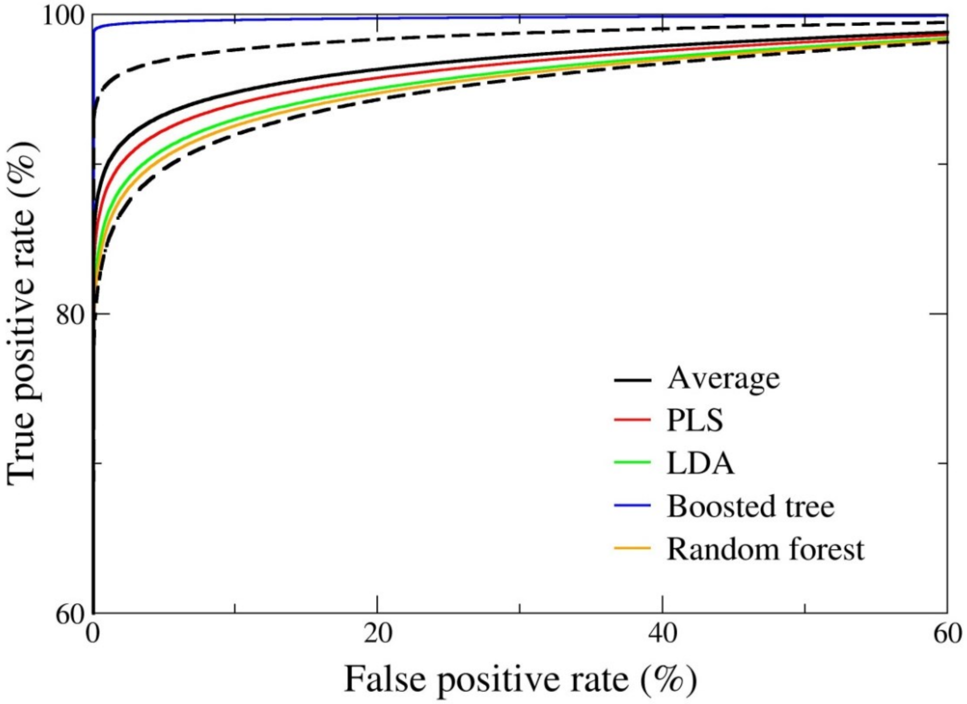
True positive rate (%)
False positive rate (%)
Average
PLS
LDA
Boosted tree
Random forest